Int Ophthalmol (2022) 42:455–467
https://doi.org/10.1007/s10792-021-02062-y

ORIGINAL PAPER

Sensitivity and specificity of MultiColor imaging in detecting proliferative diabetic retinopathy

Sara Vaz-Pereira · Tiago Morais-Sarmento · Gabriella De Salvo

Received: 10 May 2021 / Accepted: 21 September 2021 / Published online: 26 October 2021
© The Author(s), under exclusive licence to Springer Nature B.V. 2021

Abstract

Purpose To evaluate the accuracy of MultiColor imaging (MC) compared to fluorescein angiography (FA) in detecting proliferative diabetic retinopathy (PDR) and associated diabetic retinopathy features.

Methods Fifty-nine eyes from 38 PDR patients were included. MC images were reviewed by 2 independent masked graders. A qualitative analysis based on the following features was performed: neovascular complexes (NVC), disc neovascularization (NVD), neovascularization elsewhere (NVE), microaneurysm (MA), intraretinal hemorrhage (IRH), vitreous hemorrhage (VH), preretinal hemorrhage (PRH), fibrosis, hard exudates (HE), epiretinal membrane (ERM), diabetic macular edema (DME), ischemia and laser spots (LS). Measures of diagnostic accuracy compared to FA were determined.

Results The sensitivity for the detection of NVC using MC was 95.1%, with a specificity of 40.0%, positive predictive value (PPV) of 92.9% and negative predictive value (NPV) of 50.0%. Sensitivity and specificity were higher in detecting NVD (88.9% and 76.9%) while NVE registered higher PPV (88.9%). MC was highly sensitive in detecting IRH, HE, ERM and LS (100%), MA (98.0%) and fibrosis (95.5%). Highest specificity was found for VH (100.0%), DME (100.0%), PRH (98.1%) and LS (89.5%). The area under the receiver-operating characteristic analysis of MC was excellent in NVD (0.83, 95% confidence interval (CI), 0.71–0.95, $p < 0.001$), IRH (0.89, 95% CI 0.74–1.00, $p < 0.001$), VH (0.81, 95% CI 0.60–1.00, $p = 0.005$) and PRH (0.89, 95% CI 0.68–1.00, $p = 0.004$) and outstanding in LS detection (0.95, 95% CI 0.87–1.00, $p < 0.001$). These results are likely due to the contrast and quality of the MC since better discrimination is enabled by the green wavelength.

Conclusion MC is useful in evaluation of PDR patients and can complement noninvasive imaging. MC detected some PDR features more accurately than FA such as NVD, IRH, VH, PRH, and LS.

Keywords Diabetic retinopathy · Diagnostic imaging · Fluorescein angiography · MultiColor

S. Vaz-Pereira (✉)
Department of Ophthalmology, Centro Hospitalar Universitário de Lisboa Norte, EPE - Hospital de Santa Maria, Avenida Professor Egas Moniz, 1649-035 Lisbon, Portugal
e-mail: saravazpereira@gmail.com

S. Vaz-Pereira
Department of Ophthalmology, Faculdade de Medicina, Universidade de Lisboa, Lisbon, Portugal

T. Morais-Sarmento
Department of Ophthalmology, Hospital do Espírito Santo de Évora EPE, Évora, Portugal

G. De Salvo
Southampton Eye Unit, University Hospital Southampton Foundation Trust, Southampton, UK

imaging · Proliferative diabetic retinopathy · Retinal neovascularization

Abbreviations

AUC	Area under the receiver-operating characteristics
CI	Confidence interval
CFP	Color fundus photographs
DM	Diabetes mellitus
DME	Diabetic macular edema
DR	Diabetic retinopathy
ERM	Epiretinal membrane
FA	Fluorescein angiography
HE	Hard exudates
ILM	Internal limiting membrane
IRH	Intraretinal hemorrhage
IRMA	Intraretinal microvasculature abnormalities
LS	Laser spots
MA	Microaneurysm
MC	MultiColor imaging
NIR	Near-infrared reflectance
NPV	Negative predictive value
NVC	Neovascular complex
NVD	Neovascularization of the disc
NVE	Neovascularization elsewhere
OCT	Optical coherence tomography
PDR	Proliferative diabetic retinopathy
PPV	Positive predictive value
PRH	Preretinal hemorrhage
PRP	Panretinal photocoagulation
ROC	Receiver-operating characteristic
VEGF	Vascular endothelial growth factor
VH	Vitreous hemorrhage

Introduction

Diabetic retinopathy (DR) is a leading cause of blindness [1, 2]. By 2030, the World Health Organization estimates the prevalence of DM to reach 366 million adult patients and DR is estimated to affect 191 million [2]. This emphasizes the need for appropriate and early screening and, thus, the screening programs need to become as effective as possible [3]. Also, patient flow needs to be optimized in clinics with obtention of more information from less testing or without moving patients to different machines and/or rooms, which can be very time-consuming. This has become even more significant with the COVID-19 pandemic which has created a new healthcare reality.

MultiColor scanning laser imaging (MC) is a recent non-invasive modality which uses 3 laser wavelengths simultaneously to obtain high-resolution en face images of the retina. The blue, green, and infrared wavelengths have different penetration ranges and thus have the ability to show structures at different depths within the retina. The blue wavelength is more useful to study the vitreoretinal interface and inner retina; the green wavelength shows details of the retinal vasculature and intraretinal features such as blood and exudation and the infrared wavelength has a higher penetration and improves visualization at the level of the outer retina, choroid and retinal pigment epithelium [4, 5].

MC presents some advantages when compared to conventional fundus examination and color fundus photography (CFP), namely (1) a superior penetration through media opacities such as cataract, (2) a better performance in undilated pupils, (3) the confocal technology blockage of scattered light offers higher resolution and higher contrast, (4) the eye-tracking technology of image stability and averaging acquisition improves resolution and (5) it is incorporated in an optical coherence tomography (OCT)/OCT and fluorescein angiography (FA) platform, not requiring the need to move to a different machine [4]. As such, this new imaging modality can identify DR pathologic changes, such as retinal neovascularization in PDR [4, 6–10].

PDR is an important cause of vision loss in diabetic individuals and is characterized by the presence of neovascular complexes (NVC) on the optic disc (NVD) or elsewhere in the retina (NVE) [11, 12]. Although there have been significant advances in imaging techniques to evaluate PDR [13, 14], FA, described in 1961 [15], is considered the gold standard to classify disease activity, guide laser therapy and evaluate treatment response. Nonetheless, it is a time-consuming invasive technique that involves intravenous administration of a fluorescein dye to obtain a vascular map of the eye and, as such, cannot be performed at every visit [16–18]. In this situation, MC may be advantageous as it can reveal retinal neovascularization undetected by CFP or funduscopy by the use of the green laser wavelength [4, 6–9]. Also, when compared to FA, MC might be a good alternative in

patients with poor quality FA or in which FA is contraindicated, due to its noninvasive character and higher penetration rate in opacities.

In this study, we evaluated the accuracy of MultiColor imaging in detecting PDR and associated DR features.

Methods

This retrospective case series included eyes from patients with PDR from the medical retina clinic at Hospital de Santa Maria, Lisbon, Portugal. This study was approved by the local ethics committee and was conducted according to the tenets of the Declaration of Helsinki. All subjects provided informed consent. Patients were identified using a database search and subsequent chart review. Exclusion criteria included other etiologies of proliferative retinopathy or reduced imaging quality due to significant media opacities.

Clinical and demographic data were collected along with same-day FA and MC images. It is our Institution's protocol to obtain MC images when performing FA. All MC images were independently evaluated by 2 trained masked medical retina specialists—SVP and GDS—with ambiguities resolved by open adjudication to decide the final grading based on previous publications on MC imaging of DR lesions [4, 6–10, 19]. The FA grading was performed openly according to the ETDRS classification from fluorescein angiograms [20, 21]. Retinal neovascularization was classified as NVE and disc neovascularization or within 1 disc diameter from its margin as NVD [22]. Other imaging features classified were: presence of round artifact [23], microaneurysm (MA), intraretinal hemorrhage (IRH), vitreous hemorrhage (VH), preretinal hemorrhage (PRH), fibrosis, hard exudates (HE), diabetic macular edema (DME), epiretinal membrane (ERM), ischemia and laser spots (LS).

High-resolution digital MC images with a field of view of 55° were obtained using Spectralis HRA with MultiColor (Heidelberg Engineering, Heidelberg, Germany). Images were captured at the time of FA and retrospectively reviewed. An initial quality check was performed and only cases with at least 10 averaged scans were included. Images were analyzed using the Heidelberg Eye Explorer (version 1.10.4.0) and the software tools were modified for improved visualization of the neovascularization in MC, respectively the color balance was changed to green–blue enhances, the noise reduction was set to low, and the sharpen function to medium [5].

Statistical analysis was performed using Microsoft Office Excel 2020 for Mac version 16.39 and SPSS version 24.0 (IBM Corp, Armonk, NY). Data were analyzed with frequency and descriptive statistics. Categorical variables were presented as counts and percentages and continuous variables as mean ± standard deviation (SD). For each feature, we calculated the sensitivity, specificity, positive predictive value (PPV), and negative predictive value (NPV), through cross-tabulation [24]. Receiver-operating characteristic (ROC) analysis was performed for several features with calculation of area under the curve (AUC) value with the respective 95% confidence interval (95%CI) and *p*-value for statistical significance compared to reference. AUC was classified as previously suggested [25, 26] and only results over 0.7 (acceptable) were included. Concordance between graders for the qualitative MC features assessed was determined with k index. The strength of agreement was considered fair from 0.21 to 0.40, moderate from 0.41 to 0.60, substantial from 0.61 to 0.80, and almost perfect from 0.81 to 1.00, as previously described [27]. P-value < 0.05 was considered statistically significant.

Results

Fifty-nine eyes from 38 individuals with a confirmed diagnosis of PDR were evaluated. The mean age ± SD was 56.6 ± 11.6, 20 (52.6%) were male, 28 (73.7%) Caucasian and 10 (26.3%) had African origin. Eight (21.1%) patients had type 1 DM and 30 (78.9%) had type 2 DM. Fifteen (39.5%) patients had bilateral disease. The affected eye was the right eye in 31 (52.5%) of cases, 2 (3.4%) eyes were treatment naïve, 42 (72.4%) received laser pan-retinal photocoagulation (PRP), 14 (24.1%) were submitted to a combination of PRP and anti-VEGF therapy and 5 (8.6%) eyes had additional surgery (pars plana vitrectomy).

Sensitivity, specificity, PPV, and NPV of MC in detecting NVC

The detection of eyes with PDR using MultiColor imaging compared to fluorescein angiography is

presented in Table 1. Thirty-nine (66.1%) NVC were identified in both MC and FA. MC identified 41 (69.5%) NVC compared to 51 (86.4%) observed in FA (Figs. 1, 2, 3). The sensitivity for the detection of NVC (NVD & NVE) using MC was 95.1%, with a specificity of 40.0%, PPV of 92.9% and NPV of 50.0%, respectively (Table 2). When considering the NVD separately from the NVE, the sensitivity, specificity, PPV, and NPV were 88.9%, 76.9%, 80.0%, and 87.0%, respectively (Table 2). NVD was identified in 30 (50.8%) eyes using MC and in 29 (49.2%) eyes using FA, with 24 (40.7%) being present in both modalities (Figs. 1, 2). For the NVE, sensitivity, specificity, PPV and NPV were, respectively, 78.0%, 63.6%, 88.9%, and 43.8% (Table 2), meaning MC and FA identified 36 (61.0%) and 46 (78.0%) complexes, respectively (Figs. 1, 2, 3). Thirty-two (54.2%) NVE was positively recognized in both techniques (Figs. 1, 2, 3).

Sensitivity, specificity, PPV and NPV of MC in detecting additional features of PDR

The data of the additional features observed is included in Tables 3 and 4. A round artifact was identified in 55 (93.2%) MC images and in none (0%) of the FA images evaluated (Fig. 3), with a specificity of 6.8% and an NPV of 100%. MA was observed in 49 (83.1%) eyes using MC and in 58 (98.3%) with FA, for a sensitivity of 98.0% and PPV of 100.0% (Fig. 2). IRH was more frequently observed in MC—40 (67.8%) versus 36 (61.0%) using FA (Fig. 2), with a sensitivity of 100.0%, specificity of 76.9%, PPV of 91.7%, and NPV of 100%. The grading of VH was quite similar between the modalities, 6 (10.2%) eyes in MC and 8 (13.6%) in FA (Fig. 3), with a specificity, specificity, PPV, and NPV of 62.5%, 100.0%, 100.0%, and 94.1%, respectively. The presence of PRH was balanced in both MC and FA – 5 (8.5%) for each – (Fig. 3), meaning a sensitivity, specificity, PPV and NPV of 80.0%, 98.1%, 80.0%, and 98.1%, correspondingly. The presence of HE had a sensitivity and NPV of 100% and specificity and PPV of 16.0% and 2.1%, respectively. HE was observed in 45 (76.3%) of

Table 1 Detection of eyes with PDR using MultiColor imaging compared to fluorescein angiography

	Fluorescein angiography			
	Positive, *n* (%)	Negative, *n* (%)	Unsure/ungradable, *n* (%)	Total, *n* (%)
MultiColor imaging				
NVC				
Positive, *n* (%)	39 (66.1)	2 (3.4)	0 (0)	41 (69.5)
Negative, *n* (%)	3 (5.1)	2 (3.4)	2 (3.4)	7 (11.9)
Unsure/ungradable, *n* (%)	9 (15.3)	1 (1.7)	1 (1.7)	11 (18.6)
Total	51 (86.4)	5 (8.5)	3 (5.1)	59 (100.0)
NVD				
Positive, *n* (%)	24 (40.7)	6 (10.2)	0 (0)	30 (50.8)
Negative, *n* (%)	3 (5.1)	20 (33.9)	1 (1.7)	24 (40.7)
Unsure/ungradable, *n* (%)	2 (3.4)	2 (3.4)	1 (1.7)	5 (8.5)
Total	29 (49.2)	28 (47.5)	2 (3.4)	59 (100.0)
NVE				
Positive, *n* (%)	32 (54.2)	4 (6.8)	0 (0)	36 (61.0)
Negative, *n* (%)	9 (15.3)	7 (11.9)	1 (1.7)	17 (28.8)
Unsure/ungradable, *n* (%)	5 (8.5)	1 (1.7)	0 (0)	6 (10.2)
Total	46 (78.0)	12 (20.3)	1 (1.7)	59 (100.0)

NVE, neovascularization elsewhere; NVD, neovascularization of the disc; PDR, proliferative diabetic retinopathy

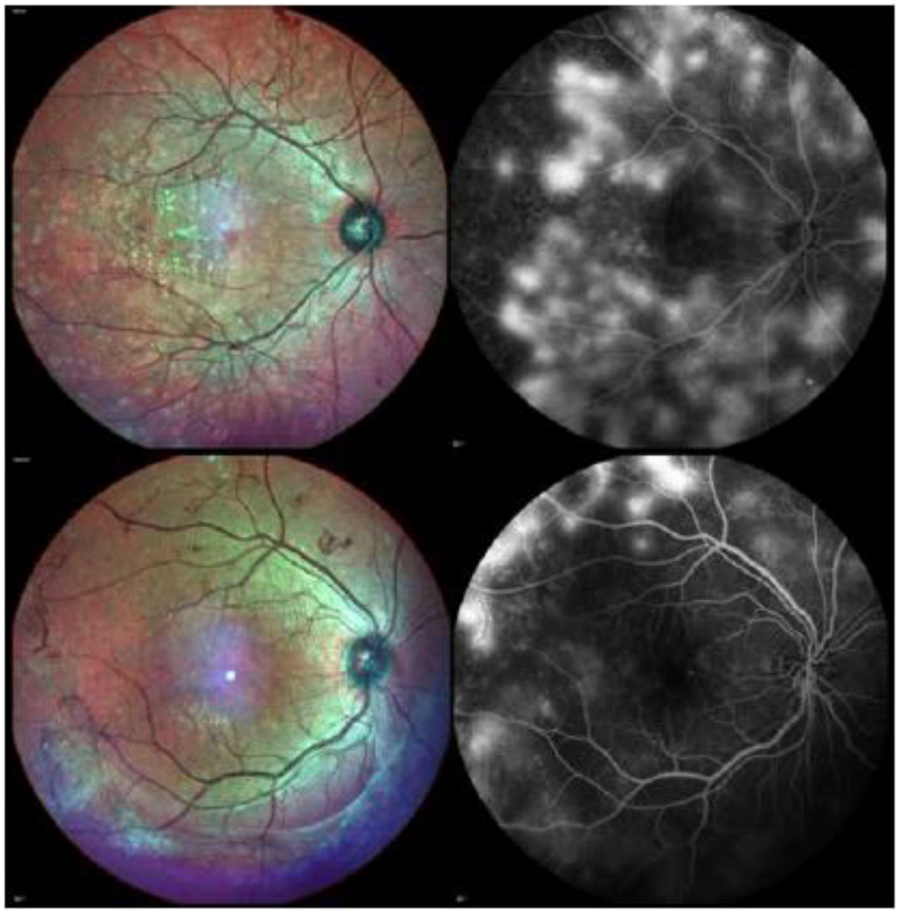

Fig. 1 Example of 2 cases of high-risk PDR. MC (top left and bottom left) showing multiple areas of NVE corresponding to areas of late leakage on matching fluorescein angiography (top right and bottom right). Note the presence of macular hard exudates in both MC images, that are not apparent in the angiogram, as well as the rounded lesions from panretinal photocoagulation (top left) and the epiretinal membrane and fibrosis along the inferotemporal arcade (bottom left)

MC image and in just one (1.7%) FA image (Fig. 1). Fibrosis was observed in 40 (67.8%) eyes in MC and in 22 (37.3%) when using FA (Fig. 1), for a specificity of 95.5%, specificity of 50.0%, PPV of 58.0%, and NPV of 93.8%. The identification of DME had a sensitivity of 45.5%, specificity of 100%, PPV of 100%, and NPV of 76.2%, being identified in 5 (8.5%) of MC and in 21 (36.1%) FAs. An ERM was found in both images in 2 (3.4%) cases, being more apparent in MC images (9; 15.3%) (Figs. 1, 2), for a sensitivity, specificity, PPV and NPV of 100.0%, 83.3%, 28.6% and 100%, respectively. Ischemia was registered in both modalities in 26 (44.1%) eyes and absent in 13 (22.0%) eyes, with disagreement between modalities in 20 (33.9%) eyes. MC presented sensitivity, specificity, PPV, and NPV values for ischemia of 74.3%, 68.4%, 81.3% and 59.1%, respectively. The observation of LS was similar between the 2 imaging modalities – 38 cases (64.4%) in MC and 37 cases (62.7%) in FA (Figs. 1, 2), reflecting a sensitivity and NPV of 100.0%, a specificity of 89.5% and PPV of 94.7%.

ROC curve of MC in detecting NVC, NVD, NVE, and other features

As shown and highlighted in bold in Table 5 the AUC analysis of MC was excellent for the detection of NVD (0.83, 95% confidence interval (CI), 0.71–0.95, $p < 0.001$), excellent for detection of VH (0.81, 95% CI 0.60–1.00, $p = 0.005$), IRH (0.89, 95% CI 0.74–1.00, $p < 0.001$) and PRH (0.89, 95% CI 0.68–1.00, $p = 0.004$) and outstanding for detection

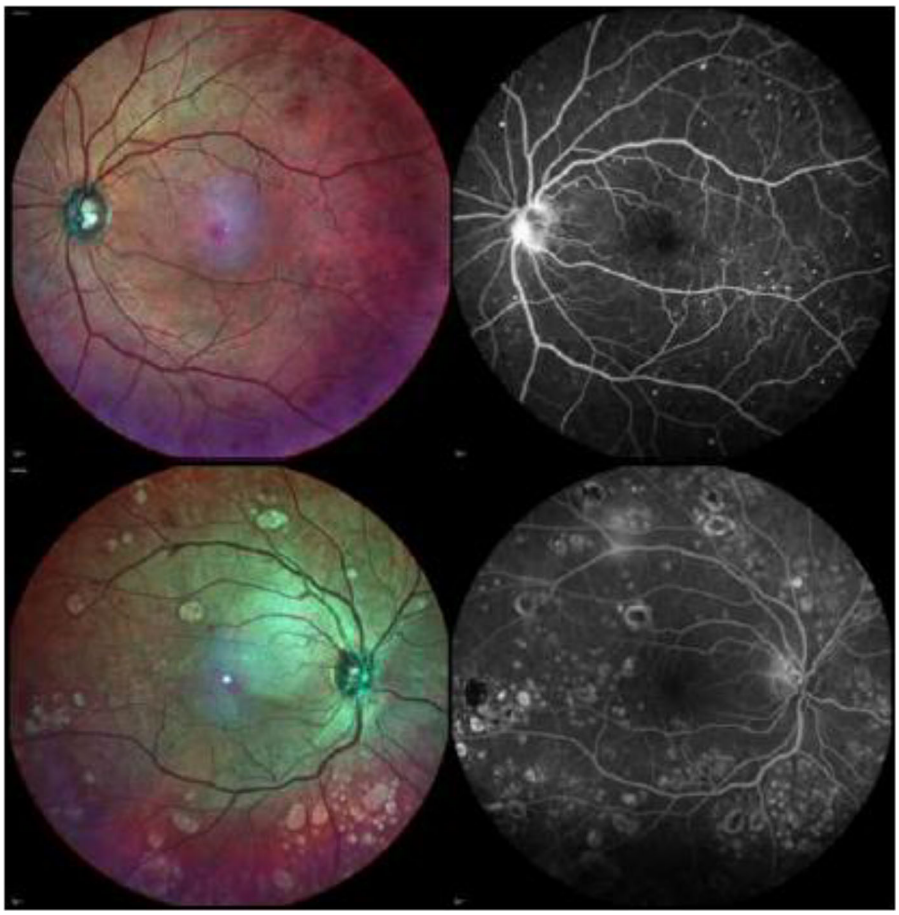

Fig. 2 Evaluation of NVD. MC showing red lesions corresponding to microaneurysms, retinal hemorrhages, and ischemia, with no apparent NVD or NVE (top left). Nevertheless, NVD can be identified in fluorescein angiography (top right), indicating PDR. On the other hand, the 2nd MC image (bottom left) clearly shows the abnormal vessels of NVD along with NVE along the superotemporal arcade, as confirmed by the angiogram (bottom, right). Note the laser scars (bottom left)

of LS (0.95, 95% CI 0.87–1.00, $p < 0.001$). This analysis also showed that MC was acceptable for the detection of NVE (0.71, 95% CI 0.53–0.89, $p = 0.035$), fibrosis (0.73, 95% CI 0.59–0.86, $p = 0.005$), and ischemia (0.71, 95% CI 0.57–0.86, $p = 0.010$). The AUC analysis for ERM detection was outstanding but without being statistically significant (0.92, 95% CI 0.81–1.00, $p = 0.052$). The AUC analysis of HE was inferior to acceptable (AUC < 0.7).

Intergrader agreement

The intergrader agreement for the MC features accessed was almost perfect with a weighted kappa of 0.86 (standard error: 0.02, 95% confidence interval: 0.82–0.88) (highlighted in bold in Table 6).

Discussion

The hallmark of PDR is the presence of neovascularization, which is induced by global retina ischemia [11, 28]. CFP and FA are still considered the gold standard for PDR although there have been recent advances in other imaging modalities [4, 6, 29–32]. The NVC is friable and can bleed, thus hemorrhagic complications such as the presence of VH or PRH are a sign of neovascularization and their presence determines the presence of high-risk PDR [22, 28, 33]. In this study, we compared the accuracy of MC to

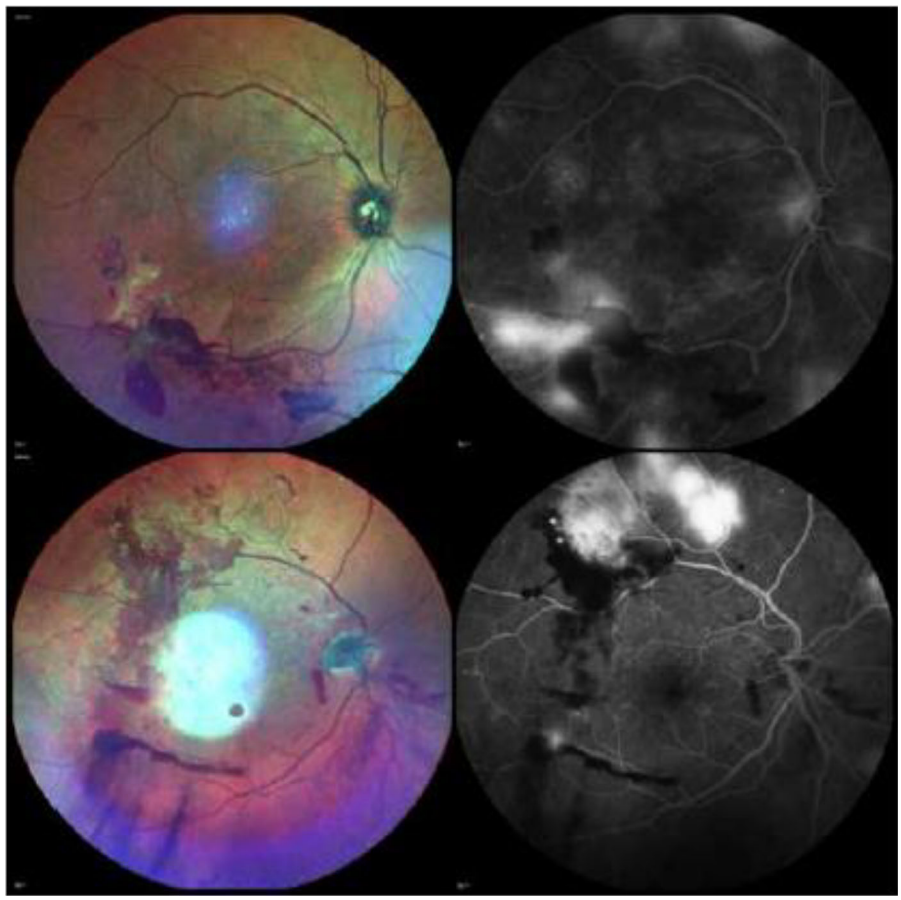

Fig. 3 Example of vitreous and preretinal hemorrhages. Preretinal hemorrhages can be easily identified in MC (top left and bottom left), as well as vitreous hemorrhages (bottom left). Note the macular striation with hard exudates from epiretinal membrane, as well as the fibrovascular NVE proliferating along the inferotemporal arcade (top left). The corresponding fluorescein angiogram (top right) shows the leakage from the NVE, as well as NVD that are not clearly apparent in the MC, but the macular changes are difficult to determine. MC image quality can be limited by the presence of a round artifact (bottom left), but in this case, it was still possible to identify the hemorrhages and abnormal vasculature. Matching angiogram (bottom right) confirms the presence of NVE and the absence of NVD

Table 2 Sensitivity and specificity of MultiColor imaging in detecting NVC, NVD and NVE

Imaging modality	Sensitivity (%)	Specificity (%)	PPV (%)	NPV (%)
MultiColor imaging				
NVC (n = 46)	95.1	40.0	92.9	50.0
NVD (n = 53)	88.9	76.9	80.0	87.0
NVE (n = 52)	78.0	63.6	88.9	43.8

NVC, neovascular complexes; NVD, neovascularization of the disc; NVE, neovascularization elsewhere; PPV, positive predictive value; NPV, negative predictive value

conventional FA to evaluate the presence of PDR and associated features. A screening test should be able to accurately identify diseased and non-diseased individuals and ideally should be highly sensitive (high probability of detecting disease) and specific (high probability of excluding the disease). However,

Table 3 Detection of eyes with additional DR features using MultiColor imaging compared to fluorescein angiography

	Fluorescein angiography			
	Positive, *n* (%)	Negative, *n* (%)	Unsure/ungradable, *n* (%)	Total, *n* (%)
MultiColor imaging				
Round Artefact				
Positive, *n* (%)	0 (0)	55 (93.2)	0 (0)	55 (93.2)
Negative, *n* (%)	0 (0)	4 (6.8)	0 (0)	4 (6.8)
Unsure/ungradable, *n* (%)	0 (0)	0 (0)	0 (0)	0 (0)
Total	0 (0)	59 (100.0)	0 (0)	59 (100.0)
Microaneurysms				
Positive, *n* (%)	49 (83.1)	0 (0)	0 (0)	49 (83.1)
Negative, *n* (%)	1 (1.7)	0 (0)	0 (0)	1 (1.7)
Unsure/ungradable, *n* (%)	8 (13.5)	0 (0)	1 (1.7)	9 (15.3)
Total	58 (98.3)	0 (0)	1 (1.7)	59 (100.0)
Intraretinal hemorrhage				
Positive, *n* (%)	33 (55.9)	3 (5.1)	4 (6.8)	40 (67.8)
Negative, *n* (%)	0 (0)	10 (16.9)	1 (1.7)	11 (18.6)
Unsure/ungradable, *n* (%)	3 (5.1)	1 (1.7)	4 (6.8)	8 (13.6)
Total	36 (61.0)	14 (23.7)	9 (15.3)	59 (100.0)
Vitreous hemorrhage				
Positive, *n* (%)	5 (8.5)	0 (0)	1 (1.7)	6 (10.2)
Negative, *n* (%)	3 (5.1)	48 (81.4)	2 (3.4)	53 (89.8)
Unsure/ungradable, *n* (%)	0 (0)	0 (0)	0 (0)	0 (0)
Total	8 (13.6)	48 (81.4)	3 (5.1)	59 (100.0)
Preretinal hemorrhage				
Positive, *n* (%)	4 (6.8)	1 (1.7)	0 (0)	5 (8.5)
Negative, *n* (%)	1 (1.7)	52 (88.1)	0 (0)	53 (89.8)
Unsure/ungradable, *n* (%)	0 (0)	1 (1.7)	0 (0)	1 (1.7)
Total	5 (8.5)	54 (91.5)	0 (0)	59 (100.0)
Fibrosis				
Positive, *n* (%)	21 (35.6)	15 (25.4)	4 (6.8)	40 (67.8)
Negative, *n* (%)	1 (1.7)	15 (25.4)	0 (0)	16 (27.1)
Unsure/ungradable, *n* (%)	0 (0.0)	2 (3.4)	1 (1.7)	3 (5.1)
Total	22 (37.3)	32 (54.2)	5 (8.5)	59 (100.0)
Hard exudates				
Positive, *n* (%)	1 (1.7)	43 (72.9)	1 (1.7)	45 (76.3)
Negative, *n* (%)	0 (0)	8 (13.6)	0 (0)	8 (13.6)
Unsure/ungradable, *n* (%)	0 (0)	6 (10.2)	0 (0)	6 (10.2)
Total	1 (1.7)	57 (96.6)	1 (1.7)	59 (100.0)
DME				
Positive, *n* (%)	5 (8.5)	0 (0)	0 (0)	5 (8.5)
Negative, *n* (%)	6 (10.2)	20 (33.9)	1 (1.7)	27 (45.8)
Unsure/ungradable, *n* (%)	10 (16.9)	16 (27.1)	1 (1.7)	27 (45.8)
Total	21 (35.6)	36 (61.0)	2 (13.4)	59 (100.0)
ERM				
Positive, *n* (%)	2 (3.4)	5 (8.5)	2 (3.4)	9 (15.3)

Table 3 continued

	Fluorescein angiography			
	Positive, *n* (%)	Negative, *n* (%)	Unsure/ungradable, *n* (%)	Total, *n* (%)
Negative, *n* (%)	0 (0)	25 (42.4)	1 (1.7)	26 (44.1)
Unsure/ungradable, *n* (%)	0 (0)	21 (35.6)	3 (5.1)	24 (40.7)
Total	2 (3.4)	51 (86.4)	6 (10.2)	59 (100.0)
Ischemia				
Positive, *n* (%)	26 (44.1)	6 (10.2)	1 (1.7)	33 (55.9)
Negative, *n* (%)	9 (15.3)	13 (22.0)	0 (0)	22 (37.3)
Unsure/ungradable, *n* (%)	3 (5.1)	0 (0)	1 (1.7)	4 (6.8)
Total	38 (64.4)	19 (32.2)	2 (3.4)	59 (100.0)
Laser spots				
Positive, *n* (%)	36 (61.0)	2 (3.4)	0 (0)	38 (64.4)
Negative, *n* (%)	0 (0)	17 (28.8)	3 (5.1)	20 (33.9)
Unsure/ungradable, *n* (%)	1 (1.7)	0 (0)	0 (0)	1 (1.7)
Total	37 (62.7)	19 (32.2)	3 (5.1)	59 (100.0)

DME, diabetic macular edema; DR, diabetic retinopathy; ERM, epiretinal membrane

Table 4 Sensitivity and specificity of MultiColor imaging in detecting additional features of DR

Imaging modality	Sensitivity (%)	Specificity (%)	PPV (%)	NPV (%)
MultiColor imaging				
Round artefact (*n* = 59)	NA	6.8	NA	100.0
Microaneurysms (*n* = 50)	98.0	NA	100.0	NA
Intraretinal hemorrhage (*n* = 46)	100.0	76.9	91.7	100.0
Vitreous hemorrhage (*n* = 56)	62.5	100.0	100.0	94.1
Preretinal hemorrhage (*n* = 58)	80.0	98.1	80.0	98.1
Fibrosis (*n* = 52)	95.5	50.0	58.0	93.8
Hard exudates (*n* = 52)	100.0	16.0	2.1	100.0
DME (*n* = 31)	45.5	100.0	100.0	76.9
ERM (*n* = 32)	100.0	83.3	28.6	100.0
Ischemia (*n* = 54)	74.3	68.4	81.3	59.1
Laser spots (*n* = 55)	100.0	89.5	94.7	100.0

DME, diabetic macular edema; ERM, epiretinal membrane; PPV, positive predictive value; NA, not applicable; NPV, negative predictive value

sensitivity and specificity are inversely proportional, which means that an increase in sensitivity will result in a decrease in specificity and vice versa [24].

We report that MC alone revealed an excellent performance in diagnosing NVCs due to its high sensitivity and PPV (very low rate of false positives), which could be helpful in diagnosing PDR, as the green reflectance highlights both the vascular and fibrotic component of neovascularization [4, 6–9]. However, MC was not so useful for PDR screening purposes due to its low specificity and NPV value, resulting in low accuracy for excluding negative cases (high rate of false negatives). We also found that the specificity and NPV were higher for NVD compared to NVE. This means that MC was able to correctly identify 76.9% of patients as having no NVD, while it properly returned a negative result for 63.6% of NVE. We believe this result may be due to better contrast in the MC image at the disc area, as the vessels are reddish and the optic disc is yellowish, and also

Table 5 Receiver-operating characteristics of MultiColor imaging in detecting NVC, NVD, NVE and additional features

MultiColor imaging	AUC (95% CI)	Discrimination [25, 26]	*p*-value
NVC (n = 46)	0.71 (0.40–1.00)	Acceptable	0.161
NVD (n = 53)	**0.83 (0.71–0.95)**	**Excellent**	**< 0.001**
NVE (n = 52)	0.71 (0.53–0.89)	Acceptable	0.035
Intraretinal hemorrhage (n = 46)	**0.89 (0.74–1.00)**	**Excellent**	**< 0.001**
Vitreous hemorrhage (n = 56)	**0.81 (0.60–1.00)**	**Excellent**	**0.005**
Preretinal hemorrhage (n = 58)	**0.89 (0.68–1.00)**	**Excellent**	**0.004**
Fibrosis (n = 52)	0.73 (0.59–0.86)	Acceptable	0.005
Hard exudates (n = 52)	0.58 (0.09–1.00)	Poor	0.790
ERM (n = 32)	0.92 (0.81–1.00)	Outstanding	0.052
Ischemia (n = 54)	0.71 (0.57–0.86)	Acceptable	0.010
Laser spots (n = 55)	**0.95 (0.87–1.00)**	**Outstanding**	**< 0.001**

AUC, area under the receiver operating characteristics; CI, confidence interval; NVC, neovascular complexes; NVD, neovascularization of the disc; NVE, neovascularization elsewhere; ERM, epiretinal membrane

Table 6 Intergrader agreement for the MultiColor features accessed

MultiColor features	k value	Strength of agreement [27]	Standard error	95% CI	*p*-value
NVC	0.66	Substantial	0.10	0.47–0.85	< 0.001
NVD	0.67	Substantial	0.08	0.52–0.83	< 0.001
NVE	0.83	Almost Perfect	0.06	0.70–0.96	< 0.001
Round artifact	0.88	Almost Perfect	0.12	0.65–1.11	< 0.001
Microaneurysms	0.94	Almost Perfect	0.06	0.83–1.05	< 0.001
Intraretinal hemorrhage	0.78	Substantial	0.08	0.70–0.87	< 0.001
Vitreous hemorrhage	0.91	Almost Perfect	0.08	0.75–1.07	< 0.001
Preretinal hemorrhage	0.90	Almost Perfect	0.10	0.71–1.09	< 0.001
Fibrosis	0.93	Almost Perfect	0.05	0.82–1.03	< 0.001
Hard exudates	0.91	Almost Perfect	0.06	0.70–0.96	< 0.001
DME	0.67	Substantial	0.08	0.52–0.82	< 0.001
ERM	0.77	Substantial	0.07	0.64–0.90	< 0.001
Ischemia	0.85	Almost Perfect	0.07	0.72–0.98	< 0.001
Laser spots	0.96	Almost Perfect	0.04	0.89–1.03	< 0.001
All features	**0.86**	**Almost Perfect**	**0.02**	**0.82–0.88**	**< 0.001**

CI, confidence interval; NVC, neovascular complexes; NVD, neovascularization of the disc; NVE, neovascularization elsewhere; DME, diabetic macular edema; ERM, epiretinal membrane

because the area of interest is much smaller, as the definition of NVD is neovascularization at or within 1 disc diameter of the disc margin [8, 22]. Indeed, the ROC analysis showed MC had excellent and statistically significant discrimination for NVD compared to FA and an only acceptable and statistically significant discrimination for NVE. This could be explained by some difficulty in distinguishing early NVE from IRMA in MC, which led to a more precise classification when using FA due to the identification of fluorescein leakage in NVE [20, 21]. Nevertheless, albeit the presence of NVE determines a more severe disease, IRMA is a known risk factor for PDR [31, 34, 35] and, in the natural disease course, about 50% of patients with severe non-proliferative DR develop PDR within a year and 15% develop high-risk

PDR [36]. Besides NVD, MC was also excellent in discriminating VH and PRH, with a higher sensitivity (80.0% vs 62.5%) for PRH and a higher specificity for VH (100% vs 98.1%). The presence of VH and PRH commonly indicates the presence of active NVC and MC was found to be statistically significant superior to FA.

Regarding other features of DR, MC was highly sensitive in detecting MA, IRH, fibrosis, and HE. These results are likely due to the contrast and quality of the images, allowing for better discrimination [4, 6–10]. Also, FA is black and white, and therefore, whitish fibrotic tissue and yellow HE are more easily unapparent in FA. MC has been reported to offer the possibility of identifying ischemic areas because of the green wavelength [4, 6, 7]. We identified the areas of nonperfusion as areas with a red enhancement when compared to the surrounding homogeneous orange background color. The ischemia appeared to be reddish and faded and could be better highlighted as hyporeflectant if seen with the blue-green wavelength filters. We found a PPV of 81.3% for ischemia and NPV of 59.1%, with acceptable discrimination in the AUC analysis. Nevertheless, MC was outstanding in the identification of laser scars from PDR treatment, with high sensitivity, specificity, PPV, and NPV.

We have demonstrated that MC has advantages over FA and it can be acquired along OCT and/or FA as it is integrated into the Heidelberg Spectralis platform (Heidelberg Engineering, Heidelberg, Germany), obviating the need to move the patient to another imaging device [4, 6], which is even more valuable as we go through the current COVID-19 pandemic. Also, our work reinforces the conclusions of other authors [4, 6, 9], that one single device allows saving time in high-volume clinics. Albeit the sensitivity was higher than the specificity when compared to FA, Roy et al. [9] validated it against CFP and so MC may be useful for diabetic screening as it can be incorporated in the Spectralis-HRA, Spectralis-OCT, or Spectralis HRA + OCT. This could be advantageous in countries that regularly perform diabetic retinal screening and are going to upgrade it with OCT. The combination of Spectralis-OCT with MC instead of separate OCT and CFP could ultimately lead to less referrals of "ungradable" cases as MC performs better in media opacities and does not require dilation [4, 6, 9]. Nonetheless, we should consider its limitations. In fact, the technique is not widely available and requires a learning curve for appropriate clinical correlation as MC incorporates 3 wavelengths, demanding a longer duration of fixation for acquisition, and the findings appear different from CFP [4, 5]. We used two trained retina specialists, familiarized with this imaging modality and thus the excellent agreement. Furthermore, the study is retrospective in nature and includes a small sample; further multicenter clinical studies are needed to complement our observations. We have chosen to compare MC to FA as the Spectralis imaging platform does not incorporate standard CFP and we stopped performing it in our routine practice. Finally, the negative impact of imaging artifacts, such as ghost maculopathy, should also be considered [4, 23]. The presence of the artifact precluded a proper assessment of macular features such as DME and ERM, which led to many cases of unsure/ungradable.

In conclusion, MC detected some PDR features such as NVD, VH, PRH, IRH, and laser spots, more accurately than FA. These findings make MC a useful test for the diagnosis and follow-up evaluation of PDR, complementing the noninvasive imaging of this disease.

Acknowledgements The authors would like to thank Sofia Sousa Mano, MD (Hospital de Santa Maria, Lisbon, Portugal) for helping in the preliminary identification of PDR patients with MultiColor images.

Authors' contribution SVP collected the data. SVP, TMS, and GDS contributed to the conception and design of the work and to data analysis and interpretation. SVP, TMS, and GDS drafted the manuscript. SVP elaborated the figures and SVP and TMS created the tables. All authors read and approved the final manuscript.

Funding None.

Data availability The data is available from the corresponding author upon reasonable request.

Declarations

Competing interest SVP reports consultant fees from Allergan, Alimera Sciences, Bayer, Novartis, and Roche, outside the submitted work. TMS has nothing to disclose. GDS reports consultant fees from Allergan, Bayer, Heidelberg Engineering and Novartis, outside the submitted work.

Animal research Not applicable.

Consent for publication All participants consented to the use of their anonymized data.

Ethics approval and consent to participate This study was approved by Centro Hospitalar Universitário de Lisboa Norte, EPE—Hospital de Santa Maria local ethics committee (Lisbon, Portugal) and was conducted in accordance with the ethical principles of the Declaration of Helsinki. Informed consent was obtained from all participants.

References

1. King H, Aubert RE, Herman WH (1998) Global burden of diabetes, 1995–2025: prevalence, numerical estimates, and projections. Diabetes Care 21(9):1414–1431. https://doi.org/10.2337/diacare.21.9.1414
2. Wild S, Roglic G, Green A, Sicree R, King H (2004) Global prevalence of diabetes: estimates for the year 2000 and projections for 2030. Diabetes Care 27(5):1047–1053. https://doi.org/10.2337/diacare.27.5.1047
3. Scanlon PH (2017) The english national screening programme for diabetic retinopathy 2003–2016. Acta Diabetol 54(6):515–525. https://doi.org/10.1007/s00592-017-0974-1
4. Tan AC, Fleckenstein M, Schmitz-Valckenberg S, Holz FG (2016) Clinical application of multicolor imaging technology. Ophthalmologica 236(1):8–18. https://doi.org/10.1159/000446857
5. GmbH HE Heidelberg Engineering Academy - SPECTRALIS MultiColor - Interpreting MultiColor images in 3 steps. https://academy.heidelbergengineering.com/course/view.php?id=204. Accessed 20 Jul 2020
6. Ahmad MSZ, Carrim ZI (2017) Multicolor scanning laser imaging in diabetic retinopathy. Optom Vis Sci 94(11):1058–1061. https://doi.org/10.1097/OPX.0000000000001128
7. Goel S, Garg B, Shah AV, Mishra S, Saurabh K, Roy R (2019) Multicolor imaging in neovascularization of disc. Indian J Ophthalmol 67(3):408. https://doi.org/10.4103/ijo.IJO_1522_18
8. Li S, Wang X, Du X, Wu Q (2018) Clinical application of multicolour scanning laser imaging in diabetic retinopathy. Lasers Med Sci 33(6):1371–1379. https://doi.org/10.1007/s10103-018-2498-5
9. Roy R, Saurabh K, Thomas NR, Chowdhury M, Shah DK (2019) Validation of multicolor imaging of diabetic retinopathy lesions vis a vis conventional color fundus photographs. Ophthalmic Surg Lasers Imaging Retina 50(1):8–15. https://doi.org/10.3928/23258160-20181212-02
10. Arrigo A, Teussink M, Aragona E, Bandello F, Battaglia Parodi M (2021) MultiColor imaging to detect different subtypes of retinal microaneurysms in diabetic retinopathy. Eye (Lond) 35(1):277–281. https://doi.org/10.1038/s41433-020-0811-6
11. Archer DB (1976) Neovascularization of the retina. Trans Ophthalmol Soc U K 96(4):471–493
12. Yau JW, Rogers SL, Kawasaki R, Lamoureux EL, Kowalski JW, Bek T, Chen SJ, Dekker JM, Fletcher A, Grauslund J, Haffner S, Hamman RF, Ikram MK, Kayama T, Klein BE, Klein R, Krishnaiah S, Mayurasakorn K, O'Hare JP, Orchard TJ, Porta M, Rema M, Roy MS, Sharma T, Shaw J, Taylor H, Tielsch JM, Varma R, Wang JJ, Wang N, West S, Xu L, Yasuda M, Zhang X, Mitchell P, Wong TY, Meta-Analysis for Eye Disease Study G (2012) Global prevalence and major risk factors of diabetic retinopathy. Diabetes Care 35 (3):556-564. doi:https://doi.org/10.2337/dc11-1909
13. Norton EW, Gutman F (1965) Diabetic retinopathy studied by fluorescein angiography. Trans Am Ophthalmol Soc 63:108–128
14. Cole ED, Novais EA, Louzada RN, Waheed NK (2016) Contemporary retinal imaging techniques in diabetic retinopathy: a review. Clin Exp Ophthalmol 44(4):289–299. https://doi.org/10.1111/ceo.12711
15. Novotny HR, Alvis DL (1961) A method of photographing fluorescence in circulating blood in the human retina. Circulation 24:82–86. https://doi.org/10.1161/01.cir.24.1.82
16. Norton EW, Gutman F (1965) Diabetic retinopathy studied by fluorescein angiography. Ophthalmologica 150(1):5–17. https://doi.org/10.1159/000304822
17. Gass JD (1968) A fluorescein angiographic study of macular dysfunction secondary to retinal vascular disease. IV. Diabetic retinal angiopathy. Arch Ophthalmol 80(5):583–591
18. Stanga PE, Papayannis A, Tsamis E, Stringa F, Cole T, D'Souza Y, Jalil A (2016) New findings in diabetic maculopathy and proliferative disease by swept-source optical coherence tomography angiography. Dev Ophthalmol 56:113–121. https://doi.org/10.1159/000442802
19. Kilic Muftuoglu I, Bartsch DU, Barteselli G, Gaber R, Nezgoda J, Freeman WR (2018) Visualization of macular pucker by multicolor scanning laser imaging. Retina 38(2):352–358. https://doi.org/10.1097/IAE.0000000000001525
20. Classification of diabetic retinopathy from fluorescein angiograms. ETDRS report number 11. Early Treatment Diabetic Retinopathy Study Research Group (1991). Ophthalmology 98 (5 Suppl):807–822
21. Focal photocoagulation treatment of diabetic macular edema. Relationship of treatment effect to fluorescein angiographic and other retinal characteristics at baseline: ETDRS report no. 19. Early Treatment Diabetic Retinopathy Study Research Group (1995). Arch Ophthalmol 113 (9):1144–1155
22. Grading diabetic retinopathy from stereoscopic color fundus photographs–an extension of the modified Airlie House classification. ETDRS report number 10. Early Treatment Diabetic Retinopathy Study Research Group (1991). Ophthalmology 98 (5 Suppl):786–806
23. Pang CE, Freund KB (2014) Ghost maculopathy: an artifact on near-infrared reflectance and multicolor imaging masquerading as chorioretinal pathology. Am J Ophthalmol 158(1):171-178.e172. https://doi.org/10.1016/j.ajo.2014.03.003
24. Parikh R, Mathai A, Parikh S, Chandra Sekhar G, Thomas R (2008) Understanding and using sensitivity, specificity and predictive values. Indian J Ophthalmol 56(1):45–50. https://doi.org/10.4103/0301-4738.37595
25. Hosmer DW, Lemeshow S (2000) Applied logistic regression, 2nd edn. Wiley, New York, pp 160–164
26. Mandrekar JN (2010) Receiver operating characteristic curve in diagnostic test assessment. J Thorac Oncol 5(9):1315–1316. https://doi.org/10.1097/JTO.0b013e3181ec173d

27. Landis JR, Koch GG (1977) The measurement of observer agreement for categorical data. Biometrics 33(1):159–174
28. Flaxel CJ, Adelman RA, Bailey ST, Fawzi A, Lim JI, Vemulakonda GA, Ying GS (2020) Diabetic retinopathy preferred practice pattern®. Ophthalmology 127(1):66–145. https://doi.org/10.1016/j.ophtha.2019.09.025
29. Tan CS, Chew MC, Lim LW, Sadda SR (2016) Advances in retinal imaging for diabetic retinopathy and diabetic macular edema. Indian J Ophthalmol 64(1):76–83. https://doi.org/10.4103/0301-4738.178145
30. Tran K, Pakzad-Vaezi K (2018) Multimodal imaging of diabetic retinopathy. Curr Opin Ophthalmol 29(6):566–575. https://doi.org/10.1097/icu.0000000000000524
31. Vaz-Pereira S, Morais-Sarmento T, Esteves Marques R (2020) Optical coherence tomography features of neovascularization in proliferative diabetic retinopathy: a systematic review. Int J Retina Vitreous 6(1):26. https://doi.org/10.1186/s40942-020-00230-3
32. Gajree S, Borooah S, Dhillon B (2017) Imaging in diabetic retinopathy: a review of current and future techniques. Curr Diabetes Rev 13(1):26–34. https://doi.org/10.2174/1573399812666151119144109
33. Early Treatment Diabetic Retinopathy Study design and baseline patient characteristics. ETDRS report number 7 (1991). Ophthalmology 98 (5 Suppl):741–756. doi:https://doi.org/10.1016/s0161-6420(13)38009-9
34. de Carlo TE, Bonini Filho MA, Baumal CR, Reichel E, Rogers A, Witkin AJ, Duker JS, Waheed NK (2016) Evaluation of preretinal neovascularization in proliferative diabetic retinopathy using optical coherence tomography angiography. Ophthalmic Surg Lasers Imaging Retina 47(2):115–119. https://doi.org/10.3928/23258160-20160126-03
35. Lee CS, Lee AY, Sim DA, Keane PA, Mehta H, Zarranz-Ventura J, Fruttiger M, Egan CA, Tufail A (2015) Reevaluating the definition of intraretinal microvascular abnormalities and neovascularization elsewhere in diabetic retinopathy using optical coherence tomography and fluorescein angiography. Am J Ophthalmol 159(1):101-110.e101. https://doi.org/10.1016/j.ajo.2014.09.041
36. Early photocoagulation for diabetic retinopathy. ETDRS report number 9. Early Treatment Diabetic Retinopathy Study Research Group (1991). Ophthalmology 98 (5 Suppl):766–785

Publisher's Note Springer Nature remains neutral with regard to jurisdictional claims in published maps and institutional affiliations.